

Coherent control of ac-driven quantum transport and minimal excitations in the fractional quantum Hall effect

Imen Taktak¹ and Inès Safi²

1: *SPEC-CEA-Saclay, CNRS/UMR 3680, F-91191, Gif-sur-Yvette, France.*

2: *Laboratoire de Physique des Solides, CNRS UMR 5802-University Paris-Saclay, France**

(Dated: February 12, 2025)

We investigate the challenges of achieving minimal excitations in the fractional quantum Hall effect and addressing Hong-Ou-Mandel -type setups under ac drives when the Tomonaga-Luttinger liquid description is adopted. We apply the unifying non-equilibrium perturbative approach to weak backscattering through a quantum point contact in a two or three terminal geometry such as the "anyon collider". We show that the photoassisted noise is always higher than the photoassisted current, thus is super-Poissonian. This is an alternative theorem to Levitov's one, violated in the TLL model, thus questioning the expression "photoassisted". In the two-terminal geometry, we analyze carefully the validity domain of the perturbative approach and the possibility to achieve the quantum regime close to frequency locking, where singularities give access to the fractional charge. Then we show the persistence of equilibrium contributions to photoassisted noise that prevent access to zero-temperature and Poissonian limits under Lorentzian pulses. Furthermore, we demonstrate that prior works on similar setups, as well as "Leviton crystallization" where the zero-temperature limit is inappropriate, may be unreliable. Our findings are also applicable to Hall interferometers, coherent conductors, and Josephson or phase-slip junctions strongly coupled to an ohmic environment under an ac bias.

I. INTRODUCTION

The Tomonaga-Luttinger (TLL) model¹ remains a central topic in both theoretical and experimental research. It serves as a paradigm for strongly correlated systems and provides a unified framework for studying various physical systems, such as edge states in the integer or fractional quantum Hall effect (FQHE)², Josephson junctions³, and coherent conductors coupled to an Ohmic environment, which have been shown to offer quantum simulations of the TLL⁴⁻⁶. While experimental evidence for its characteristic features, such as power-law behavior or the full Bethe-Ansatz solution⁷, has been inconclusive in the FQHE due to non-universal microscopic effects, it has been largely validated in quantum circuits exhibiting dynamical Coulomb blockade phenomena⁸⁻¹⁰. Among the broad range of low-energy effective models proposed for the FQHE^{11,12}—some of which represent sophisticated generalizations of the TLL model—identifying a preferred model at a given fractional filling factor ν remains challenging due to a lack of clear theoretical or experimental evidence¹³.

Despite this open theoretical issue, one of the most intriguing features of the FQHE—the fractional charge e^* of quasiparticles backscattered by an almost open quantum point contact (QPC)—has been experimentally observed¹⁴⁻¹⁶ using Poissonian non-equilibrium shot noise. Initially predicted within the TLL model^{17,18}, this Poissonian noise persists beyond the breakdown of the TLL description. This was first demonstrated in Ref.¹⁹ and later extended through the unifying non-equilibrium perturbative approach (UNEQPA)²⁰⁻²². The latter applies to a broader class of physical systems beyond tunneling junctions, without splitting the Hamiltonian, thus allowing for mutual interactions between elec-

trodes or opposite edges (see Eq.(15)). It unifies integer and fractional quantum Hall systems as well as normal and Josephson junctions (or their duals) in quantum circuits, regardless of whether the TLL model remains valid. Moreover, it can address the absence of initial thermalization, leading to a non-equilibrium distribution induced by a temperature gradient or in "anyon colliders", where the DC noise becomes super-Poissonian²³⁻²⁵ (see Eq.(8)). Within the UNEQPA to time-dependent driven systems and finite frequency noise, we have derived alternative methods for determining the fractional charge, which are more robust than Poissonian noise^{20,21,24-26}. Experimentally, such methods have been used to investigate fractional fillings ν beyond the Laughlin series, where the nature of the corresponding states has not gained unanimity^{27,28}. Addressing time-dependent voltages is also crucial for Hong-Ou-Mandel (HOM) setups designed to probe charge fractionalization²⁹⁻³¹ and statistics³²⁻³⁴. These setups fall within the scope of UNEQPA, which has been employed to interpret experimental findings in both the integer and fractional quantum Hall effects within a unified framework^{35,36}.

The independence of UNEQPA from the underlying microscopic model has been a significant advantage in all these experiments, where the measured DC current does not exhibit a clear signature of the TLL power-law behavior¹⁶, which is indeed more favorable. In fact, we will demonstrate that adopting the TLL model imposes additional constraints on UNEQPA, forbidding, for instance, taking the zero-temperature limit in the weak backscattering (WBS) regime. As a consequence, previous theoretical works on finite-frequency noise, photoassisted noise, or HOM setups obtained in this limit are not reliable. In particular, studies proposing to determine the fractional charge through peaks at resonant

values of the DC voltage using finite-frequency noise³⁷ or photoassisted noise³⁸ did not properly address their validity domain.

We also tackle the challenge of characterizing minimal excitations^{39,40} in the FQHE. In particular, we demonstrate that noise is reduced by an AC voltage superimposed on a DC voltage over a broad range of the latter. This counterintuitive behavior was previously predicted in superconductor-insulator-superconductor junctions²⁵. This contradicts Levitov's theorem (Eq.(10)), restricted to linear conductors, rendering the term 'photoassisted' unsuitable—although we retain it for consistency. Instead, we propose the term "coherent control of AC-driven quantum transport", as reflected in the title. Within the validity domain of UNEQPA, the appropriate alternative to Levitov's theorem in nonlinear conductors is a super-Poissonian photoassisted noise (Eq.(9)). This noise becomes Poissonian for an AC voltage consisting of Lorentzian pulses, provided the zero-temperature limit can be reached^{21,25}, which, however, is unattainable in the WBS regime within the TLL model—contrary to the claims of Ref.⁴¹.

Another compelling aspect of the FQHE is the anticipated anyonic statistics of fractional quasiparticles^{42–44}. Standard two-terminal HOM setups are insufficient to reveal these statistics, necessitating additional QPCs subjected to AC voltages. This setup forms the so-called "anyon collider"⁴⁵ (the terminology is not rigorous as the injected fluxes of anyons by the source QPCs are too dilute to induce collisions in the central QPC). A theoretical proposal in the DC regime⁴⁶, explicitly based on the TLL model, was successfully implemented in pioneering experiments^{44,47,48}. However, in these experiments as well, the measured DC current does not align with the expected power-law behavior. Identifying relations that reveal anyonic statistics independently of the specific model remains a major challenge. UNEQPA presents a promising approach in this direction, particularly because the "anyon collider" setup overcomes some difficulties due to TLL modelling in a two-terminal setup, as will be discussed in this paper. Notably, UNEQPA provides a robust method for extracting a key parameter λ related to anyonic statistics (see Eq.(6))²⁴.

This paper is organized as follows: The next section provides a brief review of the underlying model and some universal relations within UNEQPA. We begin by considering an arbitrary initial non-equilibrium distribution, including the "anyon collider", followed by a discussion of an initial thermal distribution, where we revisit the alternative characterization of minimal excitations. Sections three and four focus on DC and a careful study of photoassisted transport in the quantum regime, particularly near resonant values. We also explore photoconductance and photoassisted noise for AC voltage profiles given by sine waves and Lorentzian pulses, addressing the challenges in characterizing minimal excitations and strategies to avoid resonant values of the DC voltage. Furthermore, we highlight weaknesses in some prior studies.

II. APPLYING THE UNIFYING NON-EQUILIBRIUM PERTURBATIVE APPROACH (UNEQPA) TO THE FQHE

The UNEQPA encompasses a broad class of physical systems, whose Hamiltonian consists of a time-independent part, \mathcal{H}_0 , and a time-dependent component, $\mathcal{H}_B(t)$ determined by arbitrary complex function $p(t)$ and operator B ^{20–22}:

$$\mathcal{H}(t) = \mathcal{H}_0 + \mathcal{H}_B(t), \quad (1a)$$

$$\mathcal{H}_B(t) = e^{-i\omega_J t} p(t) B + e^{i\omega_J t} p^*(t) B^\dagger \quad (1b)$$

It requires however a weak observable derived from $\mathcal{H}_B(t)$, such as a charge or Josephson current, whose average and fluctuations under constant or time-dependent drives obey a set of universal relations. Sticking to charge transport, one deals with a charge current $I(t) = \partial_t Q(t)$ where Q is a charge operator that gets shifted by a charge e^* by the action of B , thus: $[B, Q] = e^* B$. Consequently one has:

$$I(t) = -i \frac{e^*}{\hbar} (e^{-i\omega_J t} p(t) B - e^{i\omega_J t} p^*(t) B^\dagger). \quad (2)$$

We focus here on incompressible chiral Hall edge states at integer or fractional filling factor ν for which \mathcal{H}_0 can include inhomogeneous and finite-range interactions. Moreover, \mathcal{H}_0 is not split into two terms, thus allows for mutual interactions between opposite edges. The initial non-equilibrium density matrix, ρ_{neq} , is arbitrary, but must commute with \mathcal{H}_0 . For Laughlin series at $\nu = 1/(2k + 1)$ with integer k , one has $e^* = \nu e$. This is not the case for ν outside the Laughlin series, as one might have many competing backscattering processes of multiple fractional values whose scaling dimensions determine their relative weight. In that case, we have to superpose the corresponding UNEQPA relation to each process (such as Eq. (4) below), and our present analysis on their validity domain is still relevant. However, if these processes have comparable dimensions, it would be difficult to discriminate experimentally between them and to use such a superposition to determine the different charges coming into play, as the methods we have deduced from the UNEQPA are aimed to determine a unique charge^{20,21}.

In fact, implementation of these methods at $\nu = 2/5$ ⁴⁹ and $\nu = 2/3$ ²⁸ permitting to give evidence for $e^* = e/5$ and $e^* = e/3$ respectively, can lead us to argue that only backscattering of a charge e^* is dominant (although the TLL model does not align with those experiments). Thus, we assume, for simplicity, that we can regroup backscattering processes with an effective amplitude Γ_B and the lowest scaling dimension $\delta < 1$, where δ is in general different from both e^*/e and ν . Notice that for co-propagating edges on each side, δ is identical to the statistical fractional phase θ/π , but can be modified by non-universal inter-edge interactions or edge reconstruction. We can then write the backscattering operator,

assumed to be localized at $x = 0$:

$$B^\dagger = \Gamma_B \Psi_u(0) \Psi_d^\dagger(0). \quad (3)$$

The quasiparticle fields are given by $\Psi_\alpha(x) = e^{i\Phi_\alpha(x)}/\sqrt{2\pi a}$ for $\alpha = u, d$, where $\Phi_u(x)$ and $\Phi_d(x)$ are upper and lower chiral bosonic fields which could be combinations of the basic edge bosonic fields. The distance cutoff a is on the order of the magnetic length. The reflection coefficient is given by $\mathcal{R} = \left[\frac{|\Gamma_B|}{\hbar v_F}\right]^2$ if we adopt a single time cutoff $\tau_0 = a/v_F$ to which corresponds an UV frequency cutoff $2\pi/\tau_0$. Notice that the time-independent Hamiltonian \mathcal{H}_0 is different within the two-terminal or the three terminal setup such as the "anyon collider", although B in Eq.(3) is similar.

A. Coherent control of ac-driven quantum transport for a non-equilibrium distribution

A crucial consequence of the UNEQPA is that for arbitrary $p(t)$ and ρ_{neq} , both the average and fluctuations of $I(t)$ at arbitrary frequencies are fully determined by two DC non-equilibrium observables that encode the signature of \mathcal{H}_0 , B , and ρ_{neq} : the DC current average, $I(\omega_J)$, and the noise, $S(\omega_J)$. Let us recall some of the relations obtained at zero frequency and specified to a periodic $p(t)$ with a frequency ω_{ph} ²⁰⁻²²:

$$O_{ph}(\omega_J) = \sum_{l=-\infty}^{l=+\infty} P_l O(\omega_J + l\omega_{ph}) \quad (4)$$

with $O = I, S$, thus O_{ph} is the average of $O(t)$ over one period $2\pi/\omega_{ph}$. Here $P_l = |p_l|^2$, with $p_l = \omega_{ph} \int_0^{2\pi/\omega_{ph}} e^{il\omega_{ph}t} p(t) dt / 2\pi$. When $|p(t)| = 1$, P_l represents the probability for the many-body eigenstates of \mathcal{H}_0 to exchange l photons with the AC sources. The current $I(\omega_J)$ is obtained from $I_{ph}(\omega_J)$ in the limit where $p(t) = 1$, in which case $p_l = \delta_l$ (the Kronecker delta). For non-periodic $p(t)$, the discrete sum is replaced by an integral, suggesting an analogy to dynamical Coulomb blockade, with a classical environment simulated by time-dependent sources^{21,22,50}.

The UNEQPA extends the Tien-Gordon theory of independent electron tunneling⁵¹⁻⁵³ to encompass strong correlations, but the side-band transmission picture must be reinterpreted in terms of many-body correlated states. The expression for the photoassisted noise in Eq. (4) applies to a HBT setup where the voltage is applied only in one reservoir, as well as to a HOM-type setup where $\omega_J = 0$ and $p(t) = e^{i[\varphi(t+\tau) - \varphi(t)]}$ with τ being the time delay between the phase $\varphi(t)$ in the left and $\varphi(t + \tau)$ in the right reservoir.

Let us also recall the Fourier transform of the current

at a finite frequency, $m\omega_{ph}$, given that $p(t)$ is periodic:

$$I_m(\omega_J) = \left(i\frac{m\omega_{ph}}{2} - \epsilon\right) \int_{-\infty}^{\infty} \frac{d\omega}{(\omega + i\epsilon)(\omega - m\omega_{ph} - i\epsilon)} \sum_{l=-\infty}^{l=+\infty} p_l^* p_{m+l} I(\omega_J + \omega + l\omega_{ph}) \quad (5)$$

where ϵ is an infinitesimal real number Eq. (4) corresponds to $m = 0$).

Let us take the example of the "anyon collider", so that the parameter ω_J of the UNEQPA is given by:

$$\omega_J = \frac{2\pi}{e^*} \sin(2\pi\lambda) I_- \quad (6)$$

where $I_- = I_u - I_d$ is the difference between the injected currents from the two QPCs sources in the upper and lower edges. λ might be given by the statistical anyonic phase, $\lambda = \theta/\pi$, but can be modified by inter-edge interactions inducing charge fractionnalisation²⁹ or by edge reconstruction⁵⁴. We have proposed a method to determine λ through finite-frequency noise in Ref.⁵⁵, independently on the underlying model, thus on the power-law behavior predicted within the TLL model. But once adopted, the latter provides explicit dc average current and noise:^{24,46}

$$I(\omega_J) = C' (\sin \pi\delta) \Im(\omega_+ + i\omega_J)^{2\delta-1} \\ S(\omega_J) = C' e^* (\cos \pi\delta) \Re(\omega_+ + i\omega_J)^{2\delta-1}, \quad (7)$$

where C' is a nonuniversal constant and $\omega_+ = 2\pi(\sin \pi\lambda)^2(I_u + I_d)/e^*$. One can inject these expressions into Eq.(4) or its equivalent formula for non-periodic $p(t)$, bypassing the difficulties we will encounter for the two-terminal geometry: the frequency ω_+ introduces an additional scale that prevents the strong backscattering regime, thereby allowing access to the zero-temperature limit. The UNEQPA, when applied to the "anyon collider", formally permits the consideration of a HOM configuration, assuming Lorentzian pulses are applied at the QPC sources to inject anyons. However, there are at least two other challenges: the nature and charge of the excitations injected from the sources, and the complex relationship between the phase $\varphi(t)$ of $p(t)$ and the potentials at the QPCs (see subsection II C and next one). Furthermore, we have verified that, by naively applying a simple sine voltage in Eq.(4), the additional finite scale ω_+ smoothes the singularities of photo-assisted transport at resonant values of ω_J , making it challenging to use it as a means of determining λ .

B. Superpoissonian photoassisted noise and Lorentzian pulses

For any non-equilibrium distribution ρ_{neq} , the universality of the super-Poissonian dc noise has been established²⁴:

$$S(\omega_J) \geq e^* |I(\omega_J)|. \quad (8)$$

This inequality holds not only in the presence of a temperature gradient but also for non-equilibrium sources at zero temperature, as in the case of the "anyon collider" (see Eq. (7)). Consequently, from Eq. (4), one can deduce the universal nature of the super-Poissonian photo-assisted noise^{21,25}:

$$S_{ph}(\omega_J) \geq e^* |I_{ph}(\omega_J)|. \quad (9)$$

The same inequality applies for non-periodic $p(t)$. This analogy with the dc case can be understood by interpreting $p(t)$ as arising from a classical environment, which can be incorporated into the dc regime.

Now, let us specify ρ_{neq} to an initial thermal distribution, $\rho_{eq} \propto e^{-\beta \mathcal{H}_0}$, at temperature $T = 1/\beta$, and explicitly express the temperature dependence of all observables O through the frequency argument $\omega_T = k_B T/\hbar$, so that O becomes a function $O(\omega_J, \omega_T)$.

Let us now specify an initial thermal distribution $\rho_{eq} \propto e^{-\beta \mathcal{H}_0}$, at a temperature $T = 1/\beta$, and explicitly express the temperature dependence of all observables O through a frequency argument $\omega_T = k_B T/\hbar$, $O(\omega_J, \omega_T)$. Then the above inequality gives a general alternative to the theorem by Levitov *et al.*³⁹, which states, in case $p(t) = e^{-i\varphi(t)}$ and $\varphi(t)$ periodic, that:

$$S_{ph}(\omega_J, \omega_T) \geq S(\omega_J, \omega_T), \quad (10)$$

for arbitrary transmission, with S reduced to Eq.(15) in the present perturbative regime. In fact, Levitov's theorem in Eq.(10) is restricted to conductors with a linear dc current, $I(\omega_J) \propto \omega_J$. We have demonstrated its breakdown in a nonlinear superconductor-insulator superconductor junction in Ref.²⁵, as well as within the TLL model in the present paper. In these two scenarios, the photo-assisted noise instead obeys the inequality in Eq.(9). Specifically, by adopting similarly $p(t) = e^{-i\varphi(t)}$ with a periodic $\varphi(t)$ in the zero-temperature limit, we have shown that Poissonian photo-assisted noise, and thus equality in Eq.(9), can only be achieved for:

$$\partial_t \varphi(t) = L(t) - n\omega_{ph}, \quad (11)$$

where $L(t)$ is formed by a series of Lorentzian pulses with width W and a dc part $\omega_J = n\omega_{ph}$.

$$L(t) = \frac{n\omega_{ph}}{\pi} \sum_{k=-\infty}^{\infty} \frac{1}{1 + (t - 2\pi k/\omega_{ph})^2/W^2}. \quad (12)$$

As will be discussed later, n does not necessarily correspond to the number of injected elementary charges per cycle²⁵, which has been imposed in Ref.³⁹ while reaching the equality in Eq.(10). In Ref.⁴¹, our general criteria for minimal excitations were incorrectly stated for the specific TLL model, where, in contrast, the photo-assisted noise remains super-Poissonian²⁵. Poissonian limit under lorentzian pulses cannot be reached neither for a non-equilibrium initial distribution, thus in the "anyon collider". This does not exclude that other ac profiles might be suitable for that. In both cases, this leaves the question of how to characterize minimal excitations still open.

C. Control of ac-drives?

Simultaneous or separate time modulation of the backscattering amplitude and the voltages is possible, whether random, non-periodic, or periodic, encoded into $p(t)$. However, the best way to the ac-drives encoded into $p(t)$ stay under control would be to apply them locally at the QPC, for instance, via a gate, which might induce amplitude modulation, $|p(t)| \neq 1$.

If instead one imposes two time-dependent potentials $V_1(t), V_2(t)$ on Gaussian or non-Gaussian QPC sources in the "anyon collider", they inject total chiral currents $I_\alpha(t)$ for $\alpha = u, d$ in the upper and lower edges, which depend, respectively, in a linear or more nonlinear way on $V_j(t)$. Then, $p(t) = e^{-i\varphi(t)}$, where $\varphi(t) = \varphi_u(t) - \varphi_d(t)$, can be determined through the equation of motion formalism for non-equilibrium bosonisation (pioneered in Ref.^{29,56}), with boundary conditions on edge $j = u, d$ given by $I_u(t), I_d(t)$ (which are operators for QPCs sources⁵⁷). Thus, the phase of $p(t)$ felt at the QPC is not local with respect to $I_\alpha(t)$:

$$\omega_{J,\alpha} + \partial_t \varphi_\alpha(t) = \int_{-\infty}^t G_\alpha(t-t') I_\alpha(t') dt'. \quad (13)$$

where we have separated the upper and lower dc Josephson frequencies, such that $\omega_{J,u} - \omega_{J,d} = \omega_J$, and the Green's function G_α , which accounts for all edges on each side $\alpha = u, d$ (see Eq.(3)), describes the propagation of plasmonic collective modes over a distance L between the reservoir and the QPC position⁵⁸. We do not express it explicitly here, as it may depend on the precise microscopic description of the edges and could be influenced by non-universal inter-edge interactions and edge reconstruction. Indeed, in the "anyon collider", average of each $I_\alpha(t)$ for $\alpha = u, d$ is obtained through a convolution with the backscattering current²⁵ at each source QPC, given by Eq.(5) for each side.

This at least indicates that preserving the shapes of $V_{1,2}(t)$, such as the Lorentzian form in Eq. (12), is far from guaranteed, particularly if ν is not a simple fraction or in the "anyon collider". This may be more feasible in a two-terminal setup and for simple fractions ν , where one expects $G_\alpha(t) = \nu \delta(t - L/v)$, assuming that the plasmon velocity v is the same on both the upper and lower edges.

III. TWO-TERMINAL SETUP: DC TRANSPORT

In this section, we address the two-terminal geometry, and specify simultaneously to an equilibrium initial distribution, and to a frequency ω_J that obeys a Josephson-type relation:

$$\omega_J = \frac{e^* V}{\hbar} \quad (14)$$

with V is the dc voltage. Then the UNEQPA yields the non-equilibrium fluctuation-dissipation relation in the

stationary regime,

$$S(\omega_J, \omega_T) = e^* \coth\left(\frac{\omega_J}{2\omega_T}\right) I(\omega_J, \omega_T), \quad (15)$$

which gives the Poissonian dc noise $S_{neq}(\omega_J) = e^* I_{neq}(\omega_J)$ at $\omega_T \ll \omega_J$ where we define $O_{neq}(\omega_J) = O(\omega_J, \omega_T \ll \omega_J)$ for $O = I, S$. It is important to note that Eq. (15) extends beyond previous works^{17,19}, which, for instance, do not account for interactions between the upper and lower edges. Therefore, within UNEQPA, time-dependent transport is fully determined by a unique function, the dc backscattering current characteristic $I(\omega_J, \omega_T)$. The transmitted current through the QPC is given by $I_0(\omega_J) - I(\omega_J, \omega_T)$ where $I_0(\omega_J) = \nu e^2 V/h = \nu e^2 \omega_J / (2\pi e^*)$.

Addressing the stationary WBS regime in the TLL model yields:

$$I(\omega_J, \omega_T) = \frac{\hbar}{e^*} \omega_J G_{eq}(\omega_T) F\left(\frac{\omega_J}{2\omega_T}\right). \quad (16)$$

Here:

$$F(y) = \frac{\sinh(y)}{y} \frac{|\Gamma(\delta + iy/\pi)|^2}{\Gamma(\delta)^2}, \quad (17)$$

where Γ is the Gamma function, and $G_{eq}(\omega_T)$ is the linear backscattering conductance in the equilibrium regime $\omega_J \ll \omega_T$:

$$G_{eq}(\omega_T) = \frac{e^{*2} \mathcal{R}}{h} \frac{\Gamma(\delta)^2}{\Gamma(2\delta)} [(2\pi)^2 \tilde{\omega}_T]^{2(\delta-1)} \quad (18)$$

From now on, we adopt the notation $\tilde{\omega} = \tau_0 \omega / 2\pi$ for all frequency scales ω . The appearance of e^{*2} is due to the renormalization of both B and ω_J by e^* (assumed to be common for simplicity). The differential backscattering conductance can be obtained from Eq.(16) :

$$G(\omega_J, \omega_T) = y G_{eq}(\omega_T) F(y) [\coth y - 2\Im(\Psi(\delta + iy/\pi))] / \pi, \quad (19)$$

where $y = \omega_J / 2\omega_T$. In the non-equilibrium limit, $\omega_T \ll \omega_J$, one gets:

$$G_{neq}(\omega_J) \simeq \mathcal{R} \frac{e^{*2}}{h} \frac{(2\pi \tilde{\omega}_J)^{2(\delta-1)}}{\Gamma(2\delta - 1)}. \quad (20)$$

We also denote by $I_{neq}(\omega_J) = I(\omega_J, \omega_T \ll \omega_J) \propto \tilde{\omega}_J^{2\delta-1}$. Let us now discuss the validity of the WBS regime in the two extreme non-equilibrium and equilibrium situations, $\omega_J \gg \omega_T$ or $\omega_J \ll \omega_T$, for which one has the power laws in Eqs.(20) or (18) respectively. In the latter, one expects that $G_{eq}(\omega_T) \ll \nu e^2/h$ as long as $\omega_T \gg \omega_B$ where ω_B refers to a crossover frequency within the Bethe-Ansatz solution to the insulating strong backscattering (SBS) regime.⁷ But if two real numbers a and b verify $a \ll b$, and given $\alpha < 0$, one has not necessarily $a^\alpha \gg b^\alpha$. Thus we prefer to impose an IR bound ω_{min} on ω_T through

the condition $G_{eq}(\omega_{min}) = \nu e^2 / 10 h$, a tenth the conductance in absence of backscattering:

$$\tilde{\omega}_{min} = \tau_0 \omega_{min} / 2\pi = \frac{1}{(2\pi)^2} \left[\frac{10 e^{*2} \Gamma(\delta)^2 \mathcal{R}}{\Gamma(2\delta) \nu e^2} \right]^{\frac{1}{2(1-\delta)}} \quad (21)$$

A similar constraint on the non-equilibrium conductance in Eq.(18) gives a different IR bound on voltage since the power law behavior has different prefactors compared to Eq.(20). Nonetheless, both IR bounds are of the same order of magnitude, thus we avoid introducing an additional cutoff, and impose that $\omega_J \geq \omega_{min}$ to ensure the non-equilibrium WBS regime. Table I gives the values $\tilde{\omega}_{min}$ for two realistic values of \mathcal{R} and two values of the scaling dimension $\delta = 1/3, 2/3$. Notice that higher values for δ might be still relevant to the FQHE (see for instance in Ref.⁵⁹) even when $\nu = 1/3 = e^*/e$. They are also relevant for dynamical Coulomb blockade as a QPC in the IQHE coupled to M edges^{4,8} is mapped to the FQHE with $\nu = \delta = M/(M+1)$; thus $M = 2$ allows to get $\delta = 2/3$, with $e^*/e = \delta$ (which modifies the value of $\tilde{\omega}_{min}$).

\mathcal{R}	$\delta = 1/3,$	$\delta = 2/3$
0.1	6×10^{-2}	1.2×10^{-2}
0.01	8×10^{-3}	4×10^{-4}

TABLE I: Values of the IR bound in units of the frequency cutoff, $\tilde{\omega}_{min} = \tau_0 \omega_{min} / 2\pi$. Thus one imposes Eq.(22) in the two equilibrium and non-equilibrium regimes to ensure that the backscattering conductance is below $\nu e^2 / 10 h$, and that the low-energy effective theory is valid. We have chosen $\nu = 1/3$ and $e^* = e\nu$.

Due to this lower bound, the non-equilibrium and equilibrium regimes where the power law is predicted might not be easily accessible. This is because one must also impose, to ensure the validity of the TLL model, that any frequency scale ω remains below the UV cutoff $2\pi/\tau_0$, ensuring $\tilde{\omega} \ll 1$. The maximum allowed frequency scale depends on non-universal features, such as the cutoff procedure or the energy range of the linearized spectrum—for instance, whether the system is graphene or a 2D gas-based FQHE system. If we assume this scale to be an order of magnitude lower, the window to observe a power-law behavior is given by:

$$\tilde{\omega}_{min} \leq \tilde{\omega} \leq 0.1, \quad (22)$$

where $\omega = \max(\omega_T, \omega_J)$. Such a window could disappear if $\tilde{\omega}_{min}$ in Eq.(21) is too high, but can be enlarged by reducing $\tilde{\omega}_{min}$ by decreasing \mathcal{R} or increasing δ or ν . For instance, both non-equilibrium and equilibrium regimes are nearly unreachable for $\mathcal{R} = 0.1$. Only at $\delta = 2/3$ and $\mathcal{R} = 0.01$ one can explore these regimes over a range of three orders of magnitude (see table I). This might explain the difficulty that arises when one looks for evidence of a power-law behavior in the FQHE over a few

orders of magnitude of temperature or dc voltages, especially in case $\delta < 1/2$. Thus one might access only to the intermediate regime where the full expression of G in Eq.(19) has to be used (see Appendix A).

IV. TWO-TERMINAL SETUP: AC-DRIVEN QUANTUM TRANSPORT

As already mentioned, robust methods for determining the charge e^* can be derived from the UNEQPA without needing knowledge of the underlying model for the edges. This is a notable advantage over the experimental works^{27,28}, which indicate a breakdown of the TLL model. Once we adopt the TLL model, and allow $p(t) \neq 1$ in Eq. (1a), we revisit the analysis of AC-driven quantum transport in the UNEQPA framework within the WBS regime. We focus on the relations obeyed by zero-frequency observables under an AC drive, such as the one in Eq. (4), which holds for HBT or HOM setups. The points of caution we address here also concern high-frequency admittance and noise, as discussed in Refs.^{20,21,24,26}.

We begin our discussion with the photo-conductance, which is the derivative of I_{ph} in Eq. (4) with respect to $V = \hbar\omega_J/e^*$.

$$G_{ph}(\omega_J; \omega_T) = \sum_{l=-\infty}^{l=+\infty} P_l G(\omega_J + l\omega_{ph}; \omega_T). \quad (23)$$

where $G(\omega_J, \omega_T)$ is given in Eq.(19). The same relation holds replacing G by S , so the same discussion applies to the photoassisted noise, denoted equally by $S_{ph}(\omega_J; \omega_T)$, while the dc noise is given by Eqs.(15),(16). One can easily understand the origin of the above formula by expanding $p(t)$ in Eqs.(1a), (3) into its Fourier components, so that one has a superposition of replica of backscattering processes with renormalized amplitudes $\Gamma_{B,l} = p_l \Gamma_B$ and effective dc biases $\omega_J + l\omega_{ph}$:

$$e^{i\omega_J t} p^*(t) B^\dagger = \sum_l \Gamma_{B,l} e^{i(\omega_J + l\omega_{ph})t} \Psi_u(0) \Psi_d^\dagger(0). \quad (24)$$

A. Validity domain and ac-driven transport

The validity of Eq.(23) requires that for each l contributing to the sum of replica, the l 'th argument on its r.h.s. must be simultaneously below the UV cutoff to be within the validity domain of the TLL model,

$$|\tilde{\omega}_J + l\tilde{\omega}_{ph}| \ll 1, \quad (25)$$

and within the WBS validity domain defined by:

$$P_l |G(\omega_J + l\omega_{ph}; \omega_T)| \leq \nu e^2 / 10 h. \quad (26)$$

A first point of caution is needed when handling large arguments that do not obey Eq. (25), at which the TLL

model breaks down. Formally, it is still legitimate to use Eq. (23), derived independently of the underlying model, thus for the expression of the dc conductance at large arguments, which is expected to deviate from the TLL expression in Eq. (19). The latter can be used only if the choice of ω_J , ω_{ph} , and $p(t)$ guarantees that one can neglect the contribution of each l that violates Eq. (25). Notice that this has to be especially checked for $\delta > 1/2$ when addressing I_{ph} , S_{ph} in the quantum regime, where large l -th terms have a power law with a positive exponent $2\delta - 1$, but this is not the case for the photoconductance in Eq. (23), where the exponent is negative, $2(\delta - 1) < 0$ (see Eq. (20)). For instance, if we fix $\omega_J = \omega_{ph}$, Lorentzian pulses in Eq. (12) with a width W large enough, such as $W\omega_{ph} = 0.25$, lead to rapidly decreasing P_l with l . For a sine voltage with $e^*V_{ac}/\hbar = \omega_{ph}$ and $|\omega_J| \leq 3\omega_{ph}$ (our choice for the majority of the figures), one can generally ignore the terms at $|l| \geq 3$.

A second point of caution is needed as one might not reach the most interesting quantum regime given by $\tilde{\omega}_T \ll \tilde{\omega}_{ph} \ll 1$, in which case we refer to the short discussion in Appendix A. One might expect that such a window is systematically opened with that for the dc stationary WBS equilibrium or non-equilibrium regime, given by Eq. (29). However, the window for $\tilde{\omega}_{ph}$ is reduced due to the additional constraints in Eqs. (25), (26) and therefore depends on the dc voltage.

A third point of caution is specific to the neighborhood of resonant values of the dc voltage $\omega_J = n \omega_{ph}$ with integer n , defined by $|\tilde{\omega}_J - n\tilde{\omega}_{ph}| \ll \tilde{\omega}_T$, where such a window becomes particularly narrow. In view of Eq. (24), the backscattering amplitude λ_{-n} experiences an effective voltage below ω_T , entering the equilibrium domain. As a result, the WBS regime remains valid only for a sufficiently high temperature compared to a renormalized IR bound that depends on each n (see also Ref.⁶⁰ for a phase-slip Josephson junction):

$$\tilde{\omega}_{min}(-n) = P_{-n}^{\frac{1}{2(1-\delta)}} \tilde{\omega}_{min}. \quad (27)$$

where $\tilde{\omega}_{min}$ is given by Eq.(21). Notice that in case $|p(t)| = 1$, thus for a constant tunneling amplitude, one has $P_{-n} < 1$ so that $\tilde{\omega}_{min}(-n) < \tilde{\omega}_{min}$. This condition can also be deduced by setting $\omega_J = n\omega_{ph}$ in Eq.(23), which leads to an unavoidable temperature-dependent term even when the dc voltage $|\omega_J = n\omega_{ph}| \gg \omega_T$ lies within the non-equilibrium domain:

$$G_{ph}(n\omega_{ph}; \omega_T) = P_{-n} G_{eq}(\omega_T) + \sum_{l \neq -n} P_l G_{neq}[(n+l)\omega_{ph}], \quad (28)$$

A similar feature arises for the finite-frequency non-equilibrium noise²⁶. The condition in Eq. (26) at $l = -n$ imposes precisely that $\tilde{\omega}_T \geq \tilde{\omega}_{min}(-n)$ (see Eq. (27)). Thus, contrary to the dc regime, the zero-temperature limit can never be taken within the WBS regime, as this drives the backscattering process with amplitude $\Gamma_{B,-n}$

(see Eq. (24)) into the strong backscattering regime, and $P_{-n}G_{eq}(\omega_T)$ would diverge.

The second term above (the truncated sum) does not depend on temperature, as G_{neq} is given by Eq.(20), but it does not dominate the first one. In fact, since $\omega_T \ll \omega_{ph}$, one has $G_{neq}[(n+l)\omega_{ph}] < G_{eq}(\omega_T)$ for any $l \neq -n$ (but not necessarily much smaller); this is because $\delta < 1$, so that $\tilde{\omega}^{2(\delta-1)}$ is a decreasing function of $\tilde{\omega}$. Therefore, we cannot neglect the equilibrium contribution to G_{ph} in Eq.(28), which also holds for $G_{ph}(\omega_J; \omega_T)$ at $|\tilde{\omega}_J - n\tilde{\omega}_{ph}| \ll \tilde{\omega}_T$.

For these reasons, a proximity of the dc voltage to a resonance might shrink or even close the window for the quantum regime. One must have (see Eqs.(25),(26)) :

$$\tilde{\omega}_{min}(-n) < \tilde{\omega}_T \ll \tilde{\omega}_{ph} \ll \min_l(|l+n|^{-1}), \quad (29)$$

where the minimum is taken over all l contributing to the sum of replica, that depends in particular on the behavior of P_l and the power-law exponent. This yields $\omega_{ph} \gg \omega_{min}(-n)$, which is however insufficient for the WBS validity of the non-equilibrium truncated sum in Eq.(28) that imposes

$$\omega_{min}(l) \leq |(n+l)\omega_{ph}|, \quad (30)$$

for each of the terms at $l \neq -n$ (see Eq. (27)). This last condition can be integrated into a stronger version of Eq. (29), once the lower bound $\tilde{\omega}_{min}(-n)$ is replaced by its maximum: $\max_l \tilde{\omega}_{min}(l)$. As an example, if $|p(t)| = 1$ and one has a sine voltage, this maximum corresponds to $l = 0$; for $e^*V_{ac} = \hbar\omega_{ph}$, the sum of replicas can be cut at $l = \pm 2$ for $|n| \leq 3$, so that the window available for ω_{ph} within the quantum regime is given by: $\tilde{\omega}_{min}(0) \ll \tilde{\omega}_{ph} \ll \min_{|l| \leq 2} (|l+n|)^{-1}$. Therefore, if we choose $\delta = 1/3$ and $\mathcal{R} = 0.1$ for which $\tilde{\omega}_{min}(0) = 0.04$ (see Eq. (27) and Table I), we cannot address the WBS regime in the vicinity of $\omega_J = 0$ nor ω_{ph} . In particular, we cannot address the HOM setup (at least for a large segment of values of the delay time τ , as will be explored in a separate publication). If we further reduce the reflection coefficient to $\mathcal{R} = 0.01$, its lowest realistic value, this permits addressing $n = 0$, thus a HOM setup, but not $\omega_J = \omega_{ph}$, which is normally important to achieve one charge per cycle for the Laughlin series. Thus, one cannot plot G_{ph} as a continuous function of the dc voltage at $\delta = 1/3$. For that, we need to consider not only a low enough $\mathcal{R} = 0.01$ but also a higher scaling dimension such as $\delta = 2/3$, ensuring a wider window for the quantum regime. Fig.1 shows the differential photo-conductance in Eq.(23) using the full expression of G in Eq.(19). It has peaks at $\omega_J = 0, \pm\omega_{ph}$ that provide a supplementary method to determine the fractional charge. It is nonetheless possible to consider the zero-temperature limit at non-resonant values of the dc voltage, as discussed in Appendix B, where we provide a simplified but stronger version of the conditions in Eqs.(25), (26).

Let us also express the photoassisted current in Eq.(4) at resonant values. Now the equilibrium term at $l = -n$

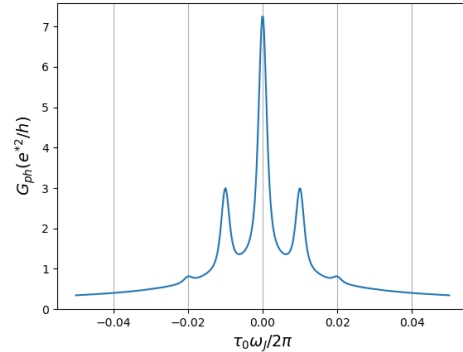


FIG. 1: The photo-conductance in the WBS regime plotted using Eqs.(23),(19) divided by $\mathcal{R}e^{*2}/h$. We take $\delta = 2/3$ and $\mathcal{R} = 10^{-2}$. We choose $\tau_0\omega_{ph}/2\pi = 0.01$. We still need to keep a finite but very small temperature, chosen here to be $\tilde{\omega}_T = 5 \times 10^{-4}$, in order to address frequency locking. The ac voltage has a sine form with an amplitude $e^*v_{ac} = \hbar\omega_{ph}$, so that $P_l = |J_l(1)|^2$.

vanishes because $I(0, \omega_T) = 0$, but taking this zero voltage limit still requires that $\omega_T \geq \omega_{min}(-n)$ in Eq.(27) in order to stay within the WBS regime. Thus, $I_{ph}(n\omega_{ph}, \omega_{min}(-n) \leq \omega_T \ll \omega_{ph})$ contains only non-equilibrium dc current terms at $l \neq -n$ in the sum given by $P_l I_{neq}[(n+l)\omega_{ph}] \propto \tilde{\omega}_{ph}^{2\delta-1}$.

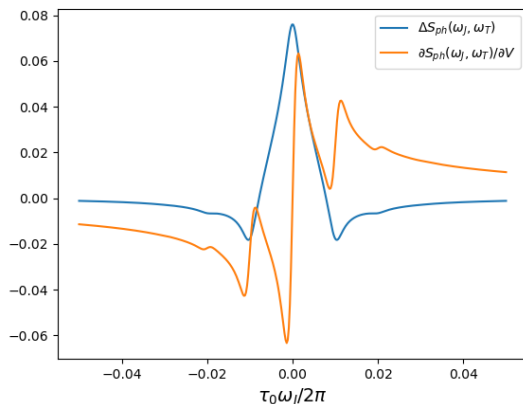


FIG. 2: Same parameters as Fig.1. The blue curve yields the excess photoassisted noise defined by subtracting the dc noise S at the same dc voltage $\Delta S_{ph}(\omega_J, \omega_T = 5 \times 10^{-4} \times 2\pi/\tau_0)$ divided by $e^{*2}\mathcal{R}/(10\tau_0)$. The orange curve corresponds to its differential with respect to V , divided by $e^{*3}\mathcal{R}/(10h)$ (thus both are dimensionless). We have used Eqs.(4),(16),(15).

The situation is different when one considers the finite frequency current $I_m(n\omega_{ph}, \omega_T)$ in Eq.(5) (we have

added the temperature argument), which still contains an equilibrium term:

$$I_m(n\omega_{ph}, \omega_T) = f_{-n,m} \tilde{\omega}_T^{2\delta-1} + \tilde{I}_m(n\omega_{ph}), \quad (31)$$

where $f_{-n,m}$ is a complex number and $\tilde{I}_m(n\omega_{ph})$ is a non-equilibrium contribution that does not depend on temperature.

Usually, reaching the quantum regime is particularly important for the photoassisted noise to eliminate any thermal fluctuations, which is unfortunately not the case in the WBS quantum regime. We obtain a form similar to Eq. (28) in the vicinity of resonant values,

$$S_{ph}(n\omega_{ph}; \omega_T) = P_{-n} S_{eq}(\omega_T) + e^* \sum_{l \neq -n} P_l |I_{neq}[(n+l)\omega_{ph}]|, \quad (32)$$

subject to the same conditions as those on the photoconductance. The first contribution of the equilibrium dc noise²⁵, given by $S_{eq}(\omega_T) = 2\omega_T G_{eq}(\omega_T)/\hbar \propto \tilde{\omega}_T^{2\delta-1}$, cannot be eliminated by considering any choice for the excess photoassisted noise as it depends on the ac voltage through P_{-n} . The plot of $\partial S_{ph}(\omega_J, \omega_T)/\partial V$ in Fig.

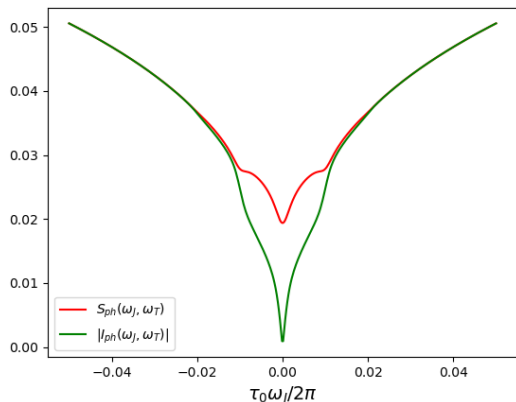


FIG. 3: Same parameters as in Fig.1. The photoassisted noise is above the absolute value of the photoassisted current, divided by $e^* \mathcal{R}/(10\tau_0)$ and $e^{*2} \mathcal{R}/(10\tau_0)$ respectively.

2, which exhibits distinct singularities at resonant values, provides an alternative method to access the fractional charge. We have also plotted the excess photo-assisted noise in the same figure, defined by subtracting the dc noise at the same dc voltage, $S(\omega_J, \omega_T)$: $\Delta S_{ph} = S_{ph} - S$. As previously shown in the case of a SIS junction²⁵, it becomes evident that $\Delta S_{ph} < 0$ for all $|\omega_J|$ above a specific threshold value, where S_{ph} equals S . This clear violation of Levitov's "theorem"³⁹ in Eq.(10) arises due to the nonlinearity of the dc current in the QPC. This further raises compelling questions about the applicability of the term "photo-assisted" noise, as it can, rather paradoxically, decrease when the QPC is irradiated with photons.

We have also carefully plotted the photo-assisted noise alongside the absolute value of the photo-assisted current in Fig.3, thus providing a solid verification of the alternative inequality in Eq.(9).

B. Lorentzian pulses

We recall that if the zero temperature limit can be reached within the validity domain of the UNEQPA, equality in Eq.(9), thus Poissonian photoassisted noise, can be reached only when $\partial_t \varphi(t) = L(t) - n\omega_{ph}$ where $L(t)$ is given by Eq.(12). Since the zero-temperature limit is impossible to reach within the WBS regime of the TLL model²⁵, the photoassisted noise generated by these Lorentzian pulses (with the subscript lor) stays super-Poissonian. It still contains the equilibrium contribution⁶¹ in Eq.(32), which cannot be neglected compared to the non-equilibrium contribution, identical to the absolute value of the photoassisted current^{21,25}:

$$S_{ph}^{lor}(n\omega_{ph}, \omega_T) = P_{-n} S_{eq}(\omega_T) + e^* |I_{ph}^{lor}(n\omega_{ph})| \quad (33)$$

Choosing $n = 1$ and $\delta = 2/3$, we see that $S_{ph}^{lor}(\omega_J = \omega_{ph}, \omega_T)$, plotted in Fig.(4) as a function of temperature, thus of $\omega_T \geq \omega_{min}$, is always above $e^* |I_{ph}^{lor}(\omega_{ph})|$. This

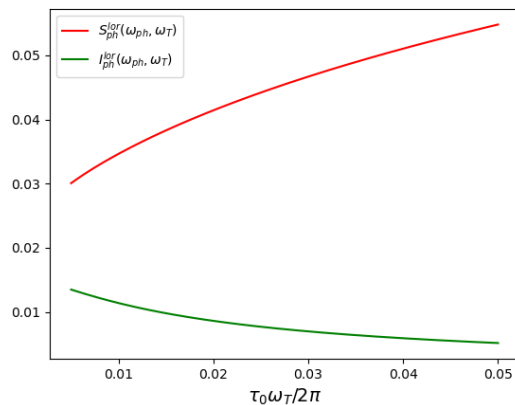


FIG. 4: The photoassisted current and noise as a function of the temperature, for lorentzian pulses with a width W given by $W\omega_{ph} = 0.25$. and $\tilde{\omega}_J = \tilde{\omega}_{ph} = 0.01$, $\delta = 2/3$ and $\mathcal{R} = 0.01$. They are divided by $e^* \mathcal{R}/(10\tau_0)$ and $e^{*2} \mathcal{R}/(10\tau_0)$ respectively. The photoassisted noise is still super-poissonian even in the quantum regime, due to the term $P_{-1} S_{eq}(\omega_T)$ (see Eq.(9)).

makes it challenging to justify that Lorentzian pulses minimize the photoassisted noise or lead to the Poissonian regime, as they are affected by thermal contributions. In fact, selecting a non-resonant value, either by adding an external dc voltage to $n\omega_{ph}$ or by altering the potential profile, provides an opportunity to reach the

zero-temperature limit. In this case, the equilibrium contribution is eliminated, potentially resulting in smaller photoassisted noise even without the need for Lorentzian pulses—a feature that warrants further investigation. Alternatively, one can also achieve a non-resonant value by prioritizing the injection of an integer number of fractional charges, as we will discuss next.

C. How to mitigate the thermal contribution to photoassisted noise?

Usually, resonant values $\omega_J = n\omega_{ph}$ ensure that an integer number of injected elementary charges ne is present per cycle. In a linear conductor where Levitov's theorem in Eq.(10) holds, minimization of the photoassisted noise imposes that n is an integer, even in the FQHE⁴⁵, thus there is no way to have an integer number of fractional charges e^* per cycle. Within the UNEQPA for non-linear conductors, the resonance values arise from ensuring the Poissonian photoassisted noise in the zero-temperature limit,²⁵ which is, however, inaccessible in the WBS regime of the TLL model. It is precisely when the function $\partial_t\varphi(t) + \omega_J$ is formed by Lorentzian pulses, where $\varphi(t)$ is the phase of $p(t) = e^{-i\varphi(t)}$ that intervenes in front of B in Eq.(1a), that we get Eq.(33). But in that case, n corresponds to the injected charges per cycle, Q_{cycle}/e ²⁵, only for simple fractions $\nu = 1/(2k+1)$. This is because Q_{cycle} is obtained by integrating the perfect linear edge current before the QPC, $I_0(t) = \nu e^2 V(t)/h$, so that, using the Josephson relationship $\omega_J = e^*V/\hbar$, one has:

$$Q_{cycle}/e = \frac{e}{h}\nu \int_0^{2\pi/\omega_{ph}} V(t)dt = \nu \frac{e\omega_J}{e^*\omega_{ph}} \quad (34)$$

Therefore, in the case of resonant values $\omega_J = n\omega_{ph}$, the injected charge per cycle is given by $Q_{cycle}/e = \nu ne/e^*$, which differs from n outside the Laughlin series for which $e^* \neq \nu e$. Let us introduce the rational r such that $\nu = re^*/e$. Then $Q_{cycle}/e = rn$, which differs from n , and may be integer or rational depending on r . However, one could also start by giving a condition on Q_{cycle} , without regard to the minimization problem or "pseudo" Poissonian regime. For instance, if r is rational, requiring that Q_{cycle}/e be an integer leads to a non-resonant value of ω_J/ω_{ph} . But even if r is integer, thus even for simple ν for which $r = 1$, one can also impose an integer number of fractional charges, $Q_{cycle} = Ne^*$, so that $\omega_J/\omega_{ph} = Ne^*/(re)$ deviates generically from resonance, thus offering the possibility to reach the zero-temperature limit as discussed before. Nonetheless, this does not ensure Eq.(33) anymore, nor minimization of the photoassisted noise in the case that the dc backscattering current was linear. Notice also that using the quantized conductance to evaluate the injected charge is not the only possibility, as one could estimate it in the reservoirs, for instance, which also gives another chance to achieve non-resonant values of ω_J/ω_{ph} .

This remark leads us to raise another important issue in case ac drives are not applied locally but from reservoirs. We have derived the non-trivial relation between the phase $\varphi(t)$ seen by the QPC and the injected chiral currents $I_{u,d}(t)$. In the "anyon collider", this leads to Eq. (6), which deviates from the Josephson-type relation in Eq. (14). However, the fractional charge in the latter could also deviate from e^* in the two-terminal geometry we address here, being instead renormalized by the non-universal parameter λ . This would make it easier to move away from resonance, thus mitigating thermal contributions.

D. Comparison to prior works

Let us now discuss a series of works on photo-assisted transport in light of our analysis. We select only some of them, but others performed within the same framework need to be checked. These works did not use the compact formula of the UNEQPA in Eq. (4), but instead employed explicit integrals, which make it more difficult to isolate, in the quantum regime and for resonant values of the dc voltage, the equilibrium term that is more transparent in our formula. It is precisely this term that leads to the divergence of the photo-assisted noise that the authors encountered in the zero-temperature limit, for instance, in Refs.^{41,62}. This divergence cannot be canceled, contrary to their claim, by any choice used in different papers for the excess photo-assisted noise by subtracting either the dc noise $S(\omega_J, \omega_T)$ (as we did in Fig. 2), the equilibrium noise $S_{eq}(\omega_T)$, or $e^* \coth(\omega_J/2\omega_T)I_{ph}(\omega_J, \omega_T)$ (in Ref.⁴¹). Such a divergence was artificially avoided in the photo-assisted current $I_{ph}(n\omega_{ph}, \omega_T)$. The latter is expressed in Eq. (4) within the UNEQPA, but we have seen that the $-n$ th term in the sum vanishes only if we take care to keep a finite temperature above Eq. (27). In fact, it is not even sufficient to avoid divergences; only valid expressions within the WBS regime can be used. Thus, one needs to impose $\omega_T \geq \omega_{min}(-n)$ in Eq. (27) when addressing the neighborhood of $\omega_J = n\omega_{ph}$.

In Ref.⁶³, a finite temperature was introduced to avoid divergences in the differential photo-assisted noise at resonant values, without discussing the infrared (IR) and ultraviolet (UV) bounds. As a result, these results do not respect the UV cutoff for the validity of the TLL model. Even if we adopt the minimum realistic value $\mathcal{R} = 0.01$, we could obtain the same curve only if we tolerate excessively high arguments in the sum of replicas.

The forbidden zero temperature limit was inappropriately taken at $n = 1$ in Ref.⁶⁴ (see the figures 3, 5, 7) and $n = 2$ in Ref.⁶⁵. In addition, the series given for photoassisted current and photoassisted noise in Refs.^{41,62,66}, based on the explicit LTL expression in Eq. (16), are not justified when, for instance, Lorentzian pulses have too small width so that P_l do not decrease fast enough, thus terms with arguments exceeding the UV cutoff are beyond the TLL's validity domain.⁶⁷

As already noted, the inequality in Eq. (9), derived first within the general framework of the UNEQPA²¹, was recovered in Ref.⁴¹ by specifying to the TLL model but expressing directly the photoassisted noise at zero temperature, which is again forbidden for the resonant values thus addressed. The authors also claim that the photoassisted noise becomes Poissonian for Lorentzian pulses, while we have shown that it stays super-Poissonian in Eq. (33), with a temperature-dependent term that diverges at zero temperature.

In fact, the reflection coefficient \mathcal{R} has often been disregarded in those works, where it disappears through the renormalization of the observables, without discussion of the ultraviolet (UV) cutoff or the infrared (IR) bounds, which nevertheless depend on \mathcal{R} . Thus, in order to discuss further the difficulty of relying on these works when carried out at $\delta = 1/3$, we choose the most favorable realistic value of the reflection coefficient, $\mathcal{R} = 10^{-2}$, which allows us to lower the IR bound as much as possible, yielding $\tilde{\omega}_{min} = 8 \times 10^{-3}$ (see Table I).

Let us first discuss works on HOM-type setups^{41,62,65,68-70} where $\omega_J = 0$ or $n = 0$. We have shown that these works cannot be addressed at $\mathcal{R} = 10^{-1}$ in the quantum regime, making the choice of $\mathcal{R} = 10^{-2}$ unavoidable. To simplify the discussion, we ignore the renormalization of the IR bound in Eq. (27), which depends on the ac voltage and time delay τ , as it does not significantly affect the order of magnitude for $n = 0$ and for most values of τ . In Ref.⁶⁸, the authors considered temperatures that are too low compared to $\tilde{\omega}_{min} = 8 \times 10^{-3}$ (see their Figure 4, where $\tilde{\omega}_T = 10^{-6}/2\pi$). A similar issue may arise in Ref.⁷⁰

Let us secondly discuss works on the finite-frequency current, or its time-dependent counterpart, shown here to contain also a temperature-dependent term even in the quantum regime through Eq. (31). We raise some doubts about the crystallization of levitons in Ref.⁶⁹. This work is based on computing the time-dependent chiral current average, which is linearly related to the backscattering current through a relation derived in Ref.²⁵ (see also Ref.⁷¹). Let us consider, for instance, Lorentzian pulses for the case $n = 5$ addressed by the authors. The infrared bound on temperature can be estimated through Eq. (27) to be $\tilde{\omega}_{min}(-n = -5) = 3 \times 10^{-4}$, which is two orders of magnitude larger compared to the temperature chosen in that work, $\tilde{\omega}_T = 10^{-5}/2\pi \simeq 10^{-6}$. This means that the carried WBS analysis is not justified even by adopting such a small reflection coefficient as 0.01.

V. CONCLUSION AND PERSPECTIVES

In this paper, we have studied quantum transport in the context of the impurity problem within the TLL model, with a particular focus on edge states in the FQHE at fractional filling factor ν . We have examined the QPC, characterized by a scaling dimension δ and a backscattering probability \mathcal{R} , and carefully analyzed the

validity of the WBS regime, which depends on these parameters as well as the low-energy effective theory. Our findings indicate that achieving the dc equilibrium or non-equilibrium regimes, where power-law behavior is expected, presents significant challenges.

Furthermore, under periodic time-dependent drives, we have explored the quantum WBS regime, which proves even more difficult to realize, particularly near resonant values of the dc voltage. A thermal contribution to the photo-assisted shot noise persists, and while this contribution becomes weak at temperatures exceeding the infrared bound, it is never negligible. Consequently, it is not possible to reach the zero-temperature limit within the WBS regime, complicating the analysis of setups such as HOM for certain parameter ranges. However, by selecting $\delta = 2/3$ and $\mathcal{R} = 0.01$, we ensure the WBS quantum regime, where both differential photoconductance and photo-assisted noise exhibit resonant peaks. This provides an alternative method for determining fractional charge. To the best of our knowledge, our derivation of the precise dc voltage dependence is novel.

Due to the thermal contribution within the TLL model, Poissonian photo-assisted noise cannot be achieved for Lorentzian pulses, as was previously predicted within the general UNEQPA framework^{21,25}. Additionally, Lorentzian pulses may not retain their shape at the QPC. We suggest that imposing an integer number of fractional charges per cycle could help avoid resonances and mitigate thermal contributions. This raises an open question regarding the characterization of minimal excitations in the FQHE. It would be interesting to explore whether non-periodic pulses, addressed within the framework of UNEQPA^{21,25,72}, could also mitigate the thermal contribution to photo-assisted noise.

We have emphasized that several studies of photo-assisted transport in TLL liquids and HOM-type setups have not sufficiently accounted for the validity criteria, leading to questionable results, particularly when addressing the zero-temperature limit at resonant values.

Finally, we note that UNEQPA is applicable to a variety of systems, including normal junctions, Josephson junctions, or dual phase-slip junctions connected to an ohmic environment^{73,74}. In the specific TLL model, the scaling dimension δ for a small Josephson junction or a good transmitting conductor connected to an ohmic environment with resistance R is given by $1/\delta = Re^2/h$, as one might deduce from Ref.³, or $1/\delta = 1 + Re^2/h$, as shown in Refs.^{4,8}. A QPC connected to M chiral edge states in the IQHE is therefore mapped to the FQHE with $\delta = M/(M + 1)$. In these specific systems, at zero temperature, resonant values, such as the centers of Shapiro steps or their duals, fall outside the scope of the UNEQPA and will be addressed in future work.

The UNEQPA provides relations obeyed by current fluctuations at finite frequencies^{21,24,26}, which are particularly relevant for studying squeezing⁷⁵ of emitted magnetoplasmons by a QPC. Adopting a TLL model gives rise to unavoidable thermal contributions in the WBS

regime, but this is not the case in the IQHE when the dc current is linear, as in Refs.^{76,77}.

Our current analysis can be extended to Fabry-Pérot interferometers^{78–80}, where fractional statistics have been revealed in the dc regime⁴³, or Mach-Zehnder interferometers, particularly in light of recent experimental progress towards the injection of Lorentzian pulses in the IQHE⁸¹ or in quantum wires⁸². It may also be relevant to plasmonic cavities with a QPC capacitively coupled to ac-driven electrodes⁸³.

Acknowledgments: The authors thank Benoit Douçot, Lucas Mazzella and M. Seddik Ouacel for inspiring discussions. They thank G. Ménard and G. Reborna for careful reading of the manuscript.

Appendix A: Intermediate regimes

First, we discuss the stationary regime when temperatures and voltages lie between the two extreme equilibrium and non-equilibrium domains. It becomes more challenging to analytically express the domain where $G(\omega_J, \omega_T) \leq \nu e^2/10h$ (see Eq. (19)). For a fixed voltage (resp. temperature), this condition provides an infrared (IR) bound on temperature (resp. voltage), which depends on ω_J (resp. ω_T), in addition to other non-universal parameters. We can show that $|G(\omega_J, \omega_T)| \leq G_{eq}(\omega_T)$ for all ω_J . Thus, whenever $\omega_T \geq \omega_{min}$ in Eq. (21), the WBS regime remains valid for all values of ω_J . Moreover, increasing ω_J lowers the IR bound on ω_T . For instance, if we take $\omega_J = 2\pi\omega_T$, the IR bound on temperature corresponds to approximately $\omega_{min}/10$ for both $\delta = 1/3$ and $\delta = 2/3$.

For time-dependent drives, we consider the case where the ac quantum WBS cannot be reached, for example, if $\tilde{\omega}_{ph} \leq \tilde{\omega}_T$. In this scenario, the first equilibrium term on the right-hand side of Eq. (28) remains, but in the second term, $G_{neq}[(n+l)\omega_{ph}]$ is replaced by the full expression $G[(n+l)\omega_{ph}; \omega_T]$ given in Eq. (19). The relatively small spacing between successive resonant values

introduces additional equilibrium terms with their associated prefactors, leading to a higher renormalized value of $\tilde{\omega}_{min}$. In the extreme regime $\omega_{ph} \ll \omega_T$, all such terms sum up to $G_{ph}(n\omega_{ph}; T) = G_{eq}(T) \sum_l P_l$. We recall that $\sum_l P_l = 1$ whenever $|p(t)| = 1$, in which case we recover the IR bound on temperature given in Eq. (21).

Appendix B: Zero-temperature limit with ac drives

Here, we qualitatively discuss the extreme zero-temperature limit. For resonant dc voltages, $\omega_J = n\omega_{ph}$, at least the term λ_{-n} in Eq. (24) undergoes a quantum transition in the dual strong backscattering regime. Although the UNEQPA framework allows one to treat strong backscattering perturbatively with respect to the dual amplitude, it is not justified to apply it to a mixture of resonant strong backscattering and nonresonant WBS terms, which will be addressed in a separate publication.

It is worth noting that the strong backscattering regime is generally less interesting, as no fractional charges are expected to tunnel. For non-resonant values of ω_J , i.e., for all effective dc voltages satisfying $|\tilde{\omega}_J + l\tilde{\omega}_{ph}| \gg \tilde{\omega}_T$, the equilibrium term is eliminated, and the system remains within the WBS regime, provided the following condition holds (see Eqs. (25), (27), and Table I).

$$\tilde{\omega}_{min}(l) \leq |\tilde{\omega}_J + l\tilde{\omega}_{ph}| \ll 1 \quad (\text{B1})$$

This also requires, in turn, that $\tilde{\omega}_{min}(l)$ are low enough to open a window in which one can insert such effective dc voltages. We can simplify such conditions in a stringer fashion as follows by imposing $\tilde{\omega}_{ph} \gg \max_l \tilde{\omega}_{min}(l)$. If we define n so that $n\omega_{ph} < \omega_J < (n+1)\omega_{ph}$, it is then sufficient to require Eq.(B1) only for $l = -n, -n-1$. Notice that only the lower bound at $l = -n$ was given in Refs.^{74,84}.

* Electronic address: ines.sa@universite-paris-saclay.fr

¹ H. J. Schulz, in *les houches revue 1d*, edited by E. Akkermans, G. Montambaux, J. Pichard, and J. Zinn-Justin (Elsevier, Amsterdam, 1995), p. 533.

² X.-G. Wen, *Int. J. Mod. Phys. B* **06**, 1711 (1992).

³ H. Grabert and G.-L. Ingold, *Europhys. Lett.* **58**, 429 (2002).

⁴ I. Safi and H. Saleur, *Phys. Rev. Lett.* **93**, 126602 (2004).

⁵ R. Zamoum, A. Crépieux, and I.Safi, *Phys. Rev. B* **85**, 125421 (2012).

⁶ A. Anthore, D.M. Kennes, E. Boulat, S. Andergassen, F. Pierre, and V. Meden, *Eur. Phys. J. Spec. Top.* **229**, 663 (2020).

⁷ P. Fendley, A. W. W. Ludwig, and H. Saleur, *Phys. Rev.*

Lett. **74**, 3005 (1995).

⁸ Jezouin, S., Albert, M., Parmentier, F. D., Anthore, A., Gennser, U., Cavanna, A., I. Safi, and Pierre, F., *Nat Commun* **4**, 1802 (2013).

⁹ A. Anthore, Z. Iftikhar, E. Boulat, F. D. Parmentier, A. Cavanna, A. Ouerghi, U. Gennser, and F. Pierre, *Phys. Rev. X* **8**, 031075 (2018).

¹⁰ H. T. Mebrahtu, I. V. Borzenets, D. E. Liu, H. Zheng, Y. V. Bomze, A. I. Smirnov, H. U. Baranger, and G. Finkelstein, *Nature* **488**, 61 (2012).

¹¹ B. Blok and X. G. Wen, *Phys. Rev. B* **42**, 8133 (1990).

¹² J. K. Jain, *Phys. Rev. Lett.* **63**, 199 (1989).

¹³ For a review, see D E Feldman and Bertrand I Halperin 2021 *Rep. Prog. Phys.* **84** 076501.

¹⁴ L. Saminadayar, D. C. Glattli, Y. Jin, and B. Etienne,

- Phys. Rev. Lett. **79**, 2526 (1997).
- ¹⁵ *Charge Fractionalization in the Integer Quantum Hall Effect*, Hiroyuki Inoue *et al*, Phys. Rev. Lett. **112**, 166801 (2014).
- ¹⁶ We also refer to a detailed analysis of the experimental results for the dc shot noise, concluding that the TLL breaks down in the NEQ regime, but seems to be valid in the equilibrium limit⁵⁹.
- ¹⁷ C. L. Kane and M. P. A. Fisher, Phys. Rev. Lett. **72**, 724 (1994).
- ¹⁸ I. Safi, Phys. Rev. B **55**, R 12 691 (1997-II).
- ¹⁹ L. S. Levitov and M. Reznikov, Phys. Rev. B **70**, 115305 (2004).
- ²⁰ I. Safi and E. V. Sukhorukov, Eur. Phys. Lett. **91**, 67008 (2010).
- ²¹ I. Safi, arxiv:1401.5950 (unpublished).
- ²² I. Safi, Phys. Rev. B **99**, 045101 (2019).
- ²³ I. Safi and H. J. Schulz, Phys. Rev. B **59**, 3040 (1999).
- ²⁴ I. Safi, Phys. Rev. B **102**, 041113 (2020).
- ²⁵ I. Safi, Phys. Rev. B **106**, 205130 (2022).
- ²⁶ B. Roussel, P. Degiovanni, and I. Safi, Phys. Rev. B **93**, 045102 (2016).
- ²⁷ M. Kapfer, P. Roulleau, I. Farrer, D. A. Ritchie, and D. C. Glattli, Science **363**, 846 (2019).
- ²⁸ R. Bisognin, H. Bartolomei, M. Kumar, I. Safi, J.-M. Berroir, E. Bocquillon, B. Plaçais, A. Cavanna, U. Gennser, Y. Jin, and G. Fève, Nature Communications **10**, 2231 (2019).
- ²⁹ I. Safi, Eur. Phys. J. B **12**, 451 (1999).
- ³⁰ V. Freulon, A. Marguerite, J. M. Berroir, B. Plaçais, A. Cavanna, Y. Jin, and G. Fève, Nat. Commun. **6**, 6854 EP (2015).
- ³¹ G. Rebola, M. Acciai, D. Ferraro, and M. Sassetti, Phys. Rev. B **101**, 245310 (2020).
- ³² M. Büttiker, Phys. Rev. Lett. **65**, 2901 (1990).
- ³³ E. Bocquillon, V. Freulon, J.-M. Berroir, P. Degiovanni, B. Plaçais, A. Cavanna, Y. Jin, and G. Fève, Science **339**, 1054 (2013).
- ³⁴ C. D. Glattli and P. S. Roulleau, Phys. Status Solidi **254**, 1600650 (2017).
- ³⁵ Imen Taktak. Phd thesis. University Paris-Saclay (2021). <https://tel.archives-ouvertes.fr/tel-03342117>.
- ³⁶ I. Taktak, M. Kapfer, J. Nath, P. Roulleau, M. Acciai, J. Splettstoesser, I. Farrer, D. A. Ritchie, and D. C. Glattli, Nat Commun **13**, 5863 (2022).
- ³⁷ C. de C. Chamon, D. E. Freed, and X. G. Wen, Phys. Rev. B **51**, 2363 (1995-II).
- ³⁸ A. Crépieux, P. Devillard, and T. Martin, Phys. Rev. B **69**, 205302 (2004).
- ³⁹ I. Klich and L. Levitov, Phys. Rev. Lett. **102**, 100502 (2009).
- ⁴⁰ J. Dubois, T. Jullien, F. Portier, P. Roche, A. Cavanna, Y. Jin, W. Wegscheider, P. Roulleau, and D. C. Glattli, Nature **502**, 659 (2013).
- ⁴¹ J. Rech, D. Ferraro, T. Jonckheere, L. Vannucci, M. Sassetti, and T. Martin, Phys. Rev. Lett. **118**, 076801 (2017).
- ⁴² P. Debray, V. N. Zverev, V. Gurevich, R. Klesse, and R. S. Newrock, Semiconductor Science and Technology **17**, R21 (2002).
- ⁴³ Nakamura, J., Liang, S., Gardner, G.C. et al. Direct observation of anyonic braiding statistics. Nat. Phys. **16**, 931–936 (2020).
- ⁴⁴ H. Bartolomei, M. Kumar, R. Bisognin, A. Marguerite, J.-M. Berroir, E. Bocquillon, B. Plaçais, A. Cavanna, Q. Dong, U. Gennser, Y. Jin, and G. Fève, Science **368**, 173 (2020).
- ⁴⁵ D. C. W. Glattli and P. Roulleau, Phys. Status Solidi B **254**, 1600650 (2017).
- ⁴⁶ B. Rosenow, I. P. Levkivskiy, and B. I. Halperin, Phys. Rev. Lett. **116**, 156802 (2016).
- ⁴⁷ P. Glidic, O. Maillet, A. Aassime, C. Piquard, A. Cavanna, U. Gennser, Y. Jin, A. Anthore, and F. Pierre, Phys. Rev. X **13**, 011030 (2023).
- ⁴⁸ M. Ruelle, E. Frigerio, J.-M. Berroir, B. Plaçais, J. Rech, A. Cavanna, U. Gennser, Y. Jin, and G. Fève, Phys. Rev. X **13**, 011031 (2023).
- ⁴⁹ L.-H. Reydellet, P. Roche, D. C. Glattli, B. Etienne, and Y. Jin, Phys. Rev. Lett. **90**, 176803 (2003).
- ⁵⁰ C. Mora, Anyonic exchange in a beam splitter, 2022.
- ⁵¹ P. K. Tien and J. R. Gordon, Phys. Rev. **129**, 647 (1961).
- ⁵² J. R. Tucker and M. J. Feldman, Rev. Mod. Phys. **57**, 1055 (1985).
- ⁵³ M. Vanević, J. Gabelli, W. Belzig, and B. Reulet, Phys. Rev. B **93**, 041416 (2016).
- ⁵⁴ R. Bhattacharyya, M. Banerjee, M. Heiblum, D. Mahalu, and V. Umansky, *Melting of interference in the fractional quantum Hall effect: Appearance of neutral modes*, arXiv:1812.06717.
- ⁵⁵ L. Privitera, N. T. Ziani, I. Safi, and B. Trauzettel, Phys. Rev. B **102**, 195413 (2020).
- ⁵⁶ I. Safi and H. J. Schulz, Phys. Rev. B **52**, 17040 (1995).
- ⁵⁷ I.P. Levkivskiy and E.V. Sukhorukov, Phys. Rev. Lett. **103**, 036801 (2009).
- ⁵⁸ I. Safi, Ann. Phys. (Paris) **22**, 463 (1997).
- ⁵⁹ N. Schiller, T. Alkalay, C. Hong, V. Umansky, M. Heiblum, Y. Oreg, and K. Snizhko, Scaling tunnelling noise in the fractional quantum Hall effect tells about renormalization and breakdown of chiral Luttinger liquid, 2024.
- ⁶⁰ D. S. Golubev and A. D. Zaikin, Phys. Rev. B **46**, 10903 (1992).
- ⁶¹ Notice that in case the complex function $p(t)$ is not known, one could access to its partial spectroscopy by varying q , as $(S_{ph}^{lor} - e^* |I_{ph}^{lor}(\omega_J, \omega_T = 0)|) / S_{eq}(\omega_T) = P_{-q}$.
- ⁶² A. Crépieux, P. Devillard, and T. Martin, Phys. Rev. B **69**, 205302 (2004).
- ⁶³ A. Crépieux, P. Devillard, and T. Martin, in *NOISE AND FLUCTUATIONS: 18th International Conference on Noise and Fluctuations - ICNF 2005*, tomás gonzález and javier mateos and daniel pardo ed. (American Inst. of Physics, Spain, 2005).
- ⁶⁴ L. Vannucci, F. Ronetti, J. Rech, D. Ferraro, T. Jonckheere, T. Martin, and M. Sassetti, Phys. Rev. B **95**, 245415 (2017).
- ⁶⁵ B. Bertin-Johannet, A. Popoff, F. Ronetti, J. Rech, T. Jonckheere, L. Raymond, B. Grémaud, and T. Martin, Phys. Rev. B **109**, 035436 (2024).
- ⁶⁶ G. Cuniberti, A. Fechner, M. Sassetti, and B. Kramer, EPL (Europhysics Letters) **48**, 66 (1999).
- ⁶⁷ L. Mazzella, M. S. Ouacel and I. Safi, unpublished.
- ⁶⁸ F. Ronetti, L. Vannucci, D. Ferraro, T. Jonckheere, J. Rech, T. Martin, and M. Sassetti, Phys. Rev. B **99**, 205406 (2019).
- ⁶⁹ F. Ronetti, L. Vannucci, D. Ferraro, T. Jonckheere, J. Rech, T. Martin, and M. Sassetti, Phys. Rev. B **98**, 075401 (2018).
- ⁷⁰ D. Ferraro, F. Ronetti, L. Vannucci, M. Acciai, J. Rech, T. Jonckheere, T. Martin, and M. Sassetti, The European

- Physical Journal Special Topics **227**, 1345 (2018).
- ⁷¹ F. Dolcini, B. Trauzettel, I. Safi, and H. Grabert, Phys. Rev. B **75**, 45332 (2007).
- ⁷² D. C. Glattli and P. Roulleau, Phys. Rev. B, 97 **12** (2018).
- ⁷³ A. G. Semenov and A. D. Zaikin, Fortschr. Phys. **65**, 1600043 (2017).
- ⁷⁴ V. D. Kurilovich, B. Remez, and L. I. Glazman, arXiv/2403.04624 (unpublished).
- ⁷⁵ J.-C. Forgues, C. Lupien, and B. Reulet, Phys. Rev. Lett. **114**, 130403 (2015).
- ⁷⁶ G. Rebora, D. Ferraro, and M. Sassetti, New Journal of Physics **23**, 063018 (2021).
- ⁷⁷ H. Bartolomei, R. Bisognin, H. Kamata, J.-M. Berroir, E. Bocquillon, G. Ménard, B. Plaçais, A. Cavanna, U. Gennser, Y. Jin, P. Degiovanni, C. Mora, and G. Fève, Phys. Rev. Lett. **130**, 106201 (2023).
- ⁷⁸ C. de C. Chamon, D. E. Freed, S. A. Kivelson, S. L. Sondhi, and X. G. Wen, Phys. Rev. B **55**, 2331 (1997).
- ⁷⁹ I. P. Levkivskiy, J. Fröhlich, and E. V. Sukhorukov, Phys. Rev. B **86**, 245105 (2012).
- ⁸⁰ D. E. Feldman and B. I. Halperin, Phys. Rev. B **105**, 165310 (2022).
- ⁸¹ H. Bartolomei *et al*, arXiv:2408.12903.
- ⁸² S. Ouacel *et al*, arXiv:2408.13025.
- ⁸³ Cano *et al*. Phys. Rev. B **88**, 165305 (2013). See also: Frigerio *et al* Commun Phys **7**, 314 (2024).
- ⁸⁴ A. V. Galaktionov, D. S. Golubev, and A. D. Zaikin, Phys. Rev. B **68**, 085317 (2003).